Nuclear Physics B347 (1990) 854–868
North-Holland

STATIC POTENTIALS AND HYBRID MESONS FROM PURE SU(3) LATTICE GAUGE THEORY

S. PERANTONIS and C. MICHAEL

Department of Applied Mathematics and Theoretical Physics, University of Liverpool, Liverpool L69 3BX, UK

Received 6 June 1990

The potentials between heavy quarks corresponding to the ground state and excited states of the gluon field are studied in pure SU(3) lattice gauge theory at $\beta = 6.0$ and $\beta = 6.2$ using blocked lattice operators. The lowest excited potential is found to correspond to the E_u symmetry of the gluon field. The relation of the results to string model predictions is discussed. The heavy quark hybrid meson spectrum in the low-lying excited potentials is evaluated for the $c\bar{c}$ and $b\bar{b}$ systems.

1. Introduction

The potential between heavy quarks, an important phenomenological feature of QCD, has been extensively studied by lattice gauge theory methods. Although the form of the ground state potential is well established, at least in the theory without dynamical fermions [1–8], the study of excited potentials, relevant to hybrid meson phenomenology, has hitherto yielded only qualitative results [9–11]. For example, controversy still pertains as to whether the lowest lying excited mode corresponds to the E_u or A_{1u} representation of the symmetry group D_{4h} of the gluonic configuration. Recently, we have been able to evaluate excited potentials in the framework of SU(2) lattice gauge theory to a high degree of accuracy [12, 13], combining the use of extended (blocked) spatial links on the lattice and multihit time-like links. In this paper we extend this work to SU(3) lattice gauge theory.

We are able to determine potentials to a high degree of accuracy compared with previous work by combining the following methods: (i) Use of blocked links in the spatial lattice direction. (ii) Use of multihit links in the temporal lattice direction. (iii) Use of more than one path to form a variational basis which enables us to determine excited potentials within a given irreducible representation of the symmetry group D_{4h} of the quark–antiquark configuration.

In our recent work on the SU(2) gauge group we have determined potentials corresponding to a large number of representations of D_{4h}. In the present work on SU(3) we confine ourselves to measuring potentials which have been found to be

relatively low lying in the SU(2) gauge group calculation, at least for some values of the quark–antiquark separation. These are the lowest potentials corresponding to the D_{4h} representations A_{1g}, E_u, A_{1u}, A_{2g}, and the first excited potential corresponding to A_{1g} (called hereinafter A'_{1g} potential). This choice is based on the assumption that the SU(2) and SU(3) potential spectra are similar. This has been found to be the case for the glueball spectra of the two gauge theories [14, 15]. The results of this paper justify this assumption for the potential spectra which we have measured for both gauge groups.

Our results show that the lowest excited mode corresponds to the E_u representation, in accordance with our SU(2) results. The values of the E_u potential are found to be in excellent agreement with the Nambu string model predictions for a range of values of the quark–antiquark separation. We solve the Schrödinger equation in this potential to obtain estimates for hybrid meson energy levels for the $c\bar{c}$ and $b\bar{b}$ systems and, in one aspect, for the $t\bar{t}$ system.

This paper is organized as follows: In sect. 2 we describe our method and provide details about our Monte Carlo evaluation of the potentials. Our results for the potentials are presented in sect. 3 and compared to string model predictions in sect. 4. Implications of the results on hybrid meson phenomenology are discussed in sect. 5. Finally, sect. 6 contains some concluding remarks.

2. The method

We use the Wilson action on L^4 lattices with periodic boundary conditions and measure correlations between linear combinations of paths transforming like suitable representations of D_{4h}, constructed from spatial links, and displaced in the time direction by a number t of lattice units. We use the notation of ref. [12] for the irreducible representations of D_{4h}: A and E correspond to minimum angular momentum about the source–antisource axis of 0 and 1 respectively in the continuum limit; the subscripts 1 (2) refer to symmetry (antisymmetry) under interchange of ends by a rotation by π about a lattice axis and g (u) refers to symmetry (antisymmetry) under interchange of ends by inversion in the midpoint.

The potential corresponding to the ground state of a given irreducible representation $\mathscr{R}$ of D_{4h} is given by the relation

$$V_0 = -a^{-1} \ln \lambda_0 = -a^{-1} \lim_{t \to \infty} \ln \left[W_{ij}(t+1)/W_{ij}(t) \right], \tag{2.1}$$

where $W_{ij}(t)$ denotes the expectation value of a Wilson loop of time extent t containing the spatial path operators O_i and O_j which transform as the representation $\mathscr{R}$, and λ_0 is the largest eigenvalue of the transfer matrix $\hat{T}$ in this representation.

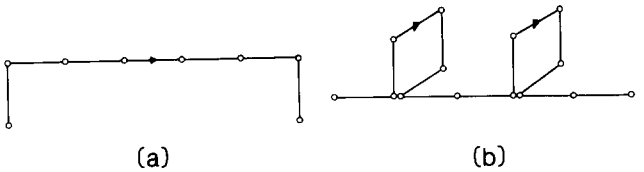

Fig. 1. Paths used to form linear combinations transforming like the irreducible representations of D_{4h}. (a) U-bend paths. The first link of the path can be in the direction of any spatial lattice vector perpendicular to the source–antisource axis. (b) These paths can have any number of square "staples" with their first link parallel to any of the spatial lattice vectors perpendicular to the source–antisource axis and the electric flux running clockwise or anticlockwise.

To reduce statistical noise in the evaluation of correlations, we use multihit temporal links [16]. This amounts to replacing links by their thermal average in the fixed environment of the six surrounding U-bends, which we evaluate numerically by a Monte Carlo simulation (typically 30 updates are used).

For finite t the ratios $\lambda(t+1,t) = W_{ij}(t+1)/W_{ij}(t)$ in eq. (2.1) receive contributions from excited states. In order to obtain reliable values for λ_0 and V_0 from relatively low values of t, we use a "blocking" algorithm [17] to create operators with high enough overlaps with the ground state. We construct linear combinations of the paths shown in fig. 1, suitably chosen to transform like each of the irreducible representations of D_{4h}. From each of the spatial paths we form new paths by replacing each spatial link by a multiple of itself plus a sum of the four neighbouring spatial U-bends,

$$U_\mu(n) \to U_\mu^1(n) = cU_\mu(n) + \sum_{\substack{\pm\nu\neq\mu \\ \nu\neq 4}} U_\nu(n)U_\mu(n+\hat{\nu})U_\nu^\dagger(n+\hat{\mu}), \qquad (2.2)$$

where c is a free parameter. We iterate this "blocking" procedure to higher levels. At each level the newly formed paths transform according to the same D_{4h} representation as the original paths. To avoid numerical overflow, which may arise from the rapid increase of the number of paths contributing to the value of a blocked link with the number of blocking iterations, we normalise the blocked link at each iteration by projecting it back to SU(3). Through the blocking process we create linear combinations of paths with spatial extension and a high overlap with the lowest lying state within a given D_{4h} representation.

The constant c in eq. (2.2) and the total number M of iterations of the blocking algorithm (blocking level) are free parameters which can be adjusted to optimize the path overlap with the lowest state in a given D_{4h} representation. For each representation, the ratio $r_{10,21} = \lambda(1,0)/\lambda(2,1)$ is a measure of the overlap with the lowest state (the larger $r_{10,21}$ the higher the overlap; if an operator overlaps only with the lowest state, the corresponding $r_{10,21}$ is equal to 1). Preliminary low

statistics studies of the representations A_{1g}, E_u and A_{1u} at $\beta = 6.0$ and 6.2 showed that with $c = 2.5$ and $c = 2.63$, respectively, we could obtain high overlaps with the ground states for all three representations for a range of values of M. The overlaps were higher than those in our SU(2) study [12, 13], which is why the statistical errors for the two studies are of similar magnitude despite the lower statistics in the present SU(3) work. For $\beta = 6.0$ we use two values M_1 and M_2 of M to create two independent paths P_{M_1} and P_{M_2} transforming according to the same group representation, and we measure the four correlations

$$C_{ij}(t) = \langle P_{M_i} | \hat{T}^t | P_{M_j} \rangle, \qquad i, j = 1, 2, \quad t = 0, 1, 2, \ldots \tag{2.3}$$

between these paths separated by t steps in the temporal direction. We analyse these correlations by a matrix variational technique to obtain, for each symmetry of the gluonic configuration, estimates for the two highest eigenvalues λ_0 and λ_1 of the transfer matrix and for the corresponding values of the potentials. This method has proved useful for obtaining information about the A'_{1g} potential, which has been found to be relatively low lying in our previous SU(2) study [12, 13].

Having obtained variational estimates $\lambda_{\text{var}}(t+1, t)$ for the eigenvalues of the transfer matrix from analysing ratios of the form $C_{ij}(t+1)/C_{ij}(t)$ at successive values of t ($t = 0, 1, 2, \ldots$), we then choose as our final estimate the value corresponding to the lowest value t_0 for which $\Delta = |\lambda_{\text{var}}(t_0 + 1, t_0) - \lambda_{\text{var}}(t_0, t_0 - 1)|$ is less than the statistical error for $\lambda_{\text{var}}(t_0 + 1, t_0)$. If the range of values of t studied is not broad enough for this to happen, Δ represents an upper systematic error in our estimate. Typical values of t_0 are $t_0 = 2$–4. Other methods of extracting a final estimate for the eigenvalues (e.g. two exponential fits) have lead to very similar results for the eigenvalues and the errors attributed to them.

We present results at two β-values ($\beta = 6.0$ and $\beta = 6.2$). The lattice sizes and details of the statistics and measured Wilson loops are presented in table 1. For $\beta = 6.0$ we have two sets of results, each for different linear combinations of the paths of fig. 1. We divide the results from each set of lattices into blocks, average the results of each block and do error analysis on the set of averages. The results

TABLE 1
Details of our Monte Carlo simulations and measurements for the potentials

β	Size of lattice	Number of updates	Lattices measured	c	Blocking levels	Range of R/a	Range of t
6.0	16^4	2×5000	2×250	2.5	18, 24	$2 \leqslant R/a \leqslant 10$	$0 \leqslant t \leqslant 5$
6.2	20^4	1500	150	2.63	50	$R/a = 2m$, $1 \leqslant m \leqslant 8$	$0 \leqslant t \leqslant 5$

of our two sets of lattices at $\beta = 6.0$ are compatible within the errors. In sect. 3 we present the results with the smallest statistical errors.

3. Results

We present results for the potentials corresponding to the lowest mode in the representations A_{1g}, E_u, A_{1u}, A_{2g} and to the first excited mode in A_{1g} at $\beta = 6.0$, and for the first three of these potentials at $\beta = 6.2$.

The ground state of the gluon field between static sources is the lowest state with A_{1g} symmetry. At a single β-value, we can fit the estimates for the potential $aV(R/a)$ using the relation

$$aV(R/a) = kR/a - 4\pi e G_L(R/a) + C, \tag{3.1}$$

with $k = \sigma a^2$, where σ represents the string tension. Here we have substituted the usual Coulomb term $-ea/R$ by a multiple of the scalar lattice propagator

$$G_L(|\boldsymbol{x}|) = \frac{1}{4L'^3} \sum_{\boldsymbol{k}} \frac{\cos(\boldsymbol{q}\cdot\boldsymbol{x})}{\sum_i \sin^2(q_i/2)},$$

$$q_i = 2\pi k_i/L', \quad -L'/2 < k_i \leqslant L'/2, \qquad i = 1,2,3, \quad L' = 3L \quad (\boldsymbol{k} \neq 0) \tag{3.2}$$

on a $(3L)^3$ lattice. This substitution has been suggested in ref. [10] as a natural way of taking into account lattice artifacts, which lead to asymmetries between on-axis and off-axis potentials. We find excellent fits to eq. (3.1) for both β-values studied. To test for scaling we fit at the two β-values simultaneously, using the same value of e and assuming that the coefficients of the linear term obey the scaling relation

$$k_{6.0}/a_{6.0}^2 = k_{6.2}/a_{6.2}^2 = \sigma. \tag{3.3}$$

We find an excellent combined fit ($\chi^2/f = 0.11$) with the values

$$\begin{aligned} &\sigma a_{6.0}^2 = 0.0476(7), \qquad a_{6.2}/a_{6.0} = 0.735(5), \qquad e = 0.277(5), \\ &C_{6.0} = 0.635(3), \qquad C_{6.2} = 0.618(3). \end{aligned} \tag{3.4}$$

The good quality of the fit confirms non-perturbative scaling for the ground state potential between the values $\beta = 6.0$ and $\beta = 6.2$. The results from the fit at $\beta = 6.0$ obtained here are compatible with previous static quark potential results [10]. Moreover, the values of the string tension and the ratio of lattice spacings obtained here are compatible with the corresponding values recently obtained in ref. [15] from the study of the glueball and torelon spectrum of SU(3) on lattices of similar size at the same β-values.

TABLE 2
Values for the ground state and excited potentials (in inverse lattice units) as a function of the quark separation for a number of D_{4h} representations at $\beta = 6.0$ and $\beta = 6.2$

R/a	A_{1g}	E_u	A_{1u}	A_{2g}	A'_{1g}
$\beta = 6.0$					
2	0.5970(6)	1.231(16)	1.286(12)	1.45(4)	1.33(3, − 8)
3	0.6993(13)	1.221(14)	1.302(13)	1.47(5)	1.38(2, − 6)
4	0.7722(24)	1.225(14)	1.327(14)	1.49(6)	1.40(2, − 6)
5	0.8329(35)	1.233(13)	1.357(15)	1.50(8)	1.44(3, − 4)
6	0.8888(48)	1.251(13)	1.395(19)	1.52(3, − 6)	1.48(3)
7	0.9428(60)	1.269(14)	1.436(20)	1.55(4)	1.53(4)
8	0.9959(71)	1.290(18)	1.463(24)	1.59(4)	1.55(4, − 6)
9	1.0475(84)	1.313(20)	1.509(25)	1.63(5)	1.58(5, − 7)
10	1.0981(99)	1.351(27)	1.571(28)	1.67(5)	1.62(6, − 9)
$\beta = 6.2$					
2	0.5336(3)	1.074(8)	1.093(8)		
4	0.6634(8)	1.055(11)	1.109(8)		
6	0.7394(19)	1.057(11)	1.142(9)		
8	0.8025(31)	1.066(11)	1.186(10)		
10	0.8611(43)	1.080(16)	1.230(13)		
12	0.9188(58)	1.106(11, − 17)	1.277(14)		
14	0.9750(77)	1.139(14, − 17)	1.324(17)		
16	1.0208(119)	1.165(17)	1.376(26)		

We can also confirm that asymptotic scaling is not achieved at the β-values we have studied: from the ratio of the lattice spacings at two neighbouring values β_1 and β_2 of β an estimate for the β-function can be obtained,

$$\beta_g = \frac{g^3}{12} \frac{\beta_2 - \beta_1}{\ln[a(\beta_2)/a(\beta_1)]} . \tag{3.5}$$

This formula gives $12g^{-3}\beta_g = -0.650(15)$ which does not agree with the value -0.885 obtained from the two-loop perturbation theory expression

$$12g^{-3}\beta_g = -\frac{33}{4\pi^2}\left(1 + \frac{51g^2}{88\pi^2}\right) \tag{3.6}$$

($g^2 = 6/\beta$) at $\beta = 6.0$. The departure from asymptotic scaling observed here is in line with Monte Carlo renormalisation group studies [5, 18] and Monte Carlo glueball spectrum and potential evaluations [10, 15].

Our estimates for the potentials corresponding to the ground state and a number of excited states of the gluon field are shown in table 2 and figs. 2 and 3 (the physical distance scale in these figures is set by the value $\sigma^{1/2} = 440$ MeV

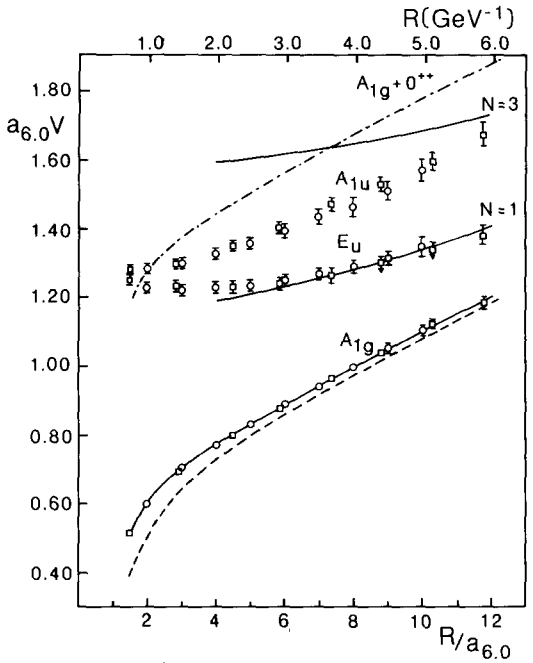

Fig. 2. The lowest A_{1g}, E_u and A_{1u} representation potentials for a static quark–antiquark pair of separation R. Results for $\beta = 6.0$ (○) and $\beta = 6.2$ (□) are plotted using the lattice spacing ratio and lattice self-energy values from a combined fit to the A_{1g} potential. Also shown are: a modified potential to take account of the possible effect of fermionic loops as discussed in sect. 5 (dashed curve); the energy of the 0^{++} glueball excitation of the ground state potential (dashed–dotted curve); and the Nambu–Goto string model potentials with $N = 1$ and $N = 3$.

determined from the $\rho, f, \ldots$ Regge trajectory). We note that the effect of using blocked paths is to increase substantially the overlap of the paths with the ground state of each representation. Typical values of $r_{10,21}$ with blocked paths are: 0.95–0.99 for A_{1g}, 0.90–0.94 for A_{1u} and E_u and 0.87–0.90 for A_{2g}. For the latter three representations these values are significantly higher than in our recent SU(2) study (at $\beta = 2.4$). As a result, we observe convergence of our estimates for the corresponding potentials at successive t-values for relatively low values of t ($t \simeq 2$–4). By contrast, the convergence of our estimates for the A'_{1g} potential is relatively poor, so that large systematic errors must be attributed to them.

Using the value for the ratio of the lattice spacings at the two β-values $\beta = 6.0$ and $\beta = 6.2$, we can check for scaling in the values of the A_{1u} and E_u potentials, for which we have results at both β-values. These are seen to scale according to the ground state scaling within the errors. This gives confidence that we are seeing continuum physics.

The gluonic configuration transforming as the E_u representation is seen from the data to be the lowest of the gluonic excitations for all the values of the

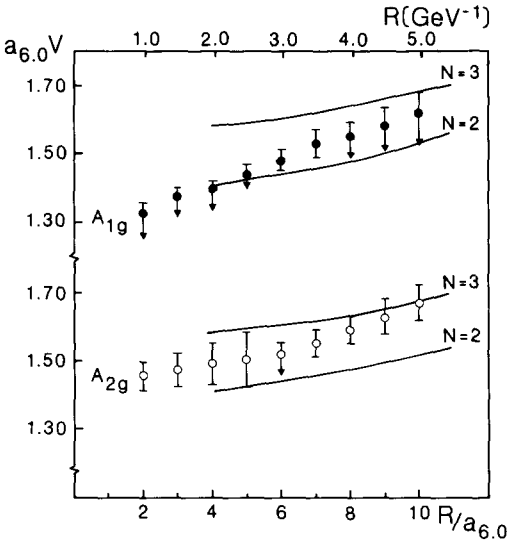

Fig. 3. The potentials corresponding to the lowest mode of the gluon field in the A_{2g} representation (○) and to the first excited mode in the A_{1g} representation (●). Results are from $\beta = 6.0$. The Nambu–Goto string potentials with $N = 2$ and $N = 3$ are also shown.

quark–antiquark separation studied. This contrasts with the results of ref. [11], where the A_{1u} potential was found to lie lower that the E_u potential. However, the results in these references were obtained by methods which tend to overestimate the E_u potential and underestimate the A_{1u} potential. In the present work, in which both potentials are statistically very well determined, we find that the two potentials are close to each other at low R and tend to diverge at larger R-values, with the E_u potential invariably the lower of the two.

It is interesting to compare the estimates for the potentials obtained here with the results of our recent heavy quark potential evaluation in SU(2) lattice gauge theory at $\beta = 2.4$ and $\beta = 2.5$. To this end we obtain a combined fit of the form given by eq. (3.1) for all values of the A_{1g} potential and for both gauge groups, assuming that an equation of the form (3.3) holds for SU(2) and SU(3) and that e has the value $\pi/12$ predicted by bosonic string models. To achieve a good fit we have to exclude the values corresponding to small R (see ref. [12] and sect. 4 of this paper). Using the appropriate estimates for the lattice spacing ratios we can plot the values for the excited potentials corresponding to both gauge groups on the same graph. It is readily seen that the ordering of the potentials for which we have results for both gauge groups is the same and the absolute values of the potentials are very similar, with the SU(3) results possibly slightly higher than the SU(2) results. This is illustrated for the potentials corresponding to the representations E_u and A_{1u} in fig. 4. Similarity between pure SU(2) and SU(3) results has

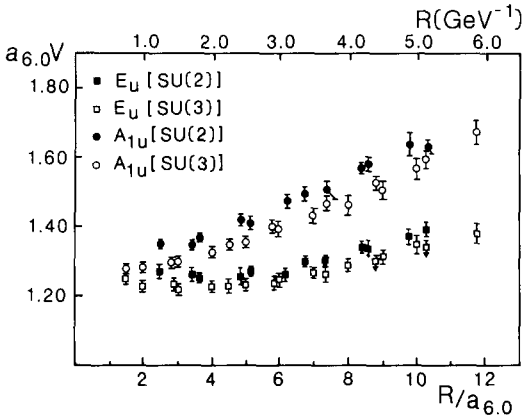

Fig. 4. Data for the E_u and A_{1u} potentials from SU(2) and SU(3) gauge theory from ref. [12] and this work are plotted here on the same graph using a combined fit to the ground state potential.

also been observed in glueball and torelon spectrum calculations [14, 15, 19]. The observed similarity between SU(2) and SU(3) results gives us confidence that in SU(3) pure gauge theory the E_u potential lies lower than all potentials which we have measured in our more complete SU(2) study.

Moreover, we can compare the E_u potential with the 0^{++} glueball excitation of the ground state potential, using the value $a_{6.0}m_{0^{++}} = 0.67(4)$ for the mass of the 0^{++} glueball obtained in ref. [15]. Fig. 2 shows that the values of the latter lie well above the values of the former. We conclude that the E_u potential lies lower than both the potentials of all D_{4h} representations for which we have results and also lower than the masses of the continuum of states lying above the ground state potential plus one 0^{++} glueball mass. This conclusion confirms the relevance of the E_u potential to the low-lying meson hybrid spectrum.

4. Comparison with string model predictions

In a string model picture of the gluon field configuration between a static quark and antiquark, the ground state potential increases linearly with the separation R at large R. Corrections to the linear behaviour originate from the zero-point motion of the quantised string. The leading correction is proportional to $1/R$ and the constant of proportionality has the universal value $-\pi/12$ [20] for a general class of bosonic string theories and $-\pi/48$ for a Dirac string. A string theory is expected to be applicable to the static quark–antiquark system for relatively large R, where the width of the flux tube is smaller than its length. At small R an effective Coulomb term dominated by one-gluon exchange also contributes to the potential. Note that in our combined fit for the ground state potential the

coefficient of the lattice $1/R$ term $-e = -0.277(5)$ is very close to the universal bosonic string value $-\pi/12 \approx -0.262$. Indeed, in order to obtain a fit with $e = \pi/12$ of similar quality to our fit of eq. (3.4) we need only exclude the data at $R_{6.0}/a_{6.0} = 2$ and $R_{6.2}/a_{6.2} = 2$. Recently, a claim has been made for a Dirac string term plus a Coulomb piece fixed by lowest-order perturbation theory [21]. This gives $e \simeq 0.15$, in disagreement with our data. However, we cannot exclude the possibility that agreement with the data could be reached if more orders of perturbation theory were included. It is thus difficult to decide about the nature of the QCD string because of the similarity in form of the Coulomb and string pieces. More definitive conclusions can be expected from a careful study of the energy of states of electric flux encircling the periodic boundary conditions, where no Coulomb piece is present [15, 19].

We now turn to the excited potentials and investigate to what extent they can be adequately described by a relativistic string model. The success of the Nambu–Goto string in describing the lowest excited static potentials has been noted in the context of a strong coupling SU(3) calculation in two dimensions [22]. Here we consider a Nambu–Goto string with fixed ends in four dimensions [23]. The corresponding potentials for the different string states are given by the formula

$$V_N = \left[\sigma^2 R^2 - \pi\sigma/6 + 2\pi N\sigma\right]^{1/2}, \qquad N = 0, 1, 2, 3, \ldots . \tag{4.1}$$

Comparison of the quantum numbers of the excited string with the continuum quantum numbers of the gluonic field configuration between fundamental sources on a hypercubic lattice gives the correspondence between the string states and the D_{4h} irreducible representations (see table 3 of ref. [12]). According to this picture, the lowest lying mode in the E_u representation corresponds to the first string excitation ($N = 1$); the lowest lying mode in the A_{2g} representation and the first excited mode in the A_{1g} representation correspond to $N = 2$; and the lowest A_{1u} mode corresponds to $N = 3$. The potentials for the relativistic Nambu–Goto string corresponding to $N = 1$, 2 and 3 are shown in figs. 2 and 3, where the value of the string tension is taken from the combined fit to the ground state potential. We note that the differences $V_N - V_0$ are essentially independent of whether we include the string fluctuation term in eq. (4.1) and not very sensitive to small variations in the value of σ.

It is clear that the $N = 1$ string potential is in excellent agreement with our lattice results for the E_u potential for separations greater than 3 GeV^{-1}. However, the string model is less successful in describing the A_{2g} potential for the values of R for which we have data. The data for the A_{1u} and A'_{1g} potentials are compatible with the string model predictions for the largest values of R studied.

The simple non-relativistic string model, where the excited potentials are equally spaced above the ground state potential with excitation energies $U_N = N\pi/R$, $N = 1, 2, \ldots$, is consistent with our E_u potential only for separations larger than 6

GeV^{-1}, while the higher excited potentials for the non-relativistic string model generally lie much higher than their lattice gauge theory counterparts for the values of R for which we have data. However, a suggestion [24] to augment the non-relativistic string model by modifying the phonon excitation energy according to the formula

$$U_1 = \frac{\pi}{R}\left[1 - \exp(-f\sigma^{1/2}R)\right], \tag{4.2}$$

to account for the finite transverse extention of the flux tube at small R, works very well for the E_u potential with $f = 0.9$ for $R \geqslant 2.5\ \mathrm{GeV}^{-1}$.

The results in this section are very much in line with what was found in SU(2) lattice gauge theory [12, 13].

5. Hybrid meson bound states

Given the relatively small statistical errors of our data for the A_{1g}, E_u and A_{1u} potentials, we are able to obtain quantitative results for the spectrum of ordinary quark model and hybrid mesons with heavy quarks and thus to improve on the qualitative results of refs. [9] and [10].

For heavy quarks the Born–Oppenheimer approximation is valid. The spectrum can be obtained by solving the Schrödinger equation for the motion of the quarks of mass m_q in the appropriate potential $V^i(R)$,

$$\left[\frac{d^2}{dR^2} + \frac{m_q}{\hbar^2}\left(E^i_{nl} - V^i(R)\right) - \frac{l(l+1) - K^2}{R^2}\right] u^i_{nl}(R) = 0, \tag{5.1}$$

where K is the angular momentum component along the inter-quark axis. The index i labels the representations of D_{4h} and $n = 1, 2, 3, \ldots$ labels the energy eigenvalues of the states with orbital angular momentum l.

Solving eq. (5.1) in the ground state (A_{1g}) potential as given by the combined fit to our data [eq. (3.4)] we obtain the spectrum for the ordinary quark model mesons, while solving in the excited potentials we obtain predictions for the energies of hybrid meson states. The quark masses are chosen to obey the relation

$$2m_q + E_0 = M_{\mathrm{exp}}, \tag{5.2}$$

where E_0 is the energy of the lowest lying state in the A_{1g} potential evaluated on the lattice and M_{exp} is the experimental value of the mass of the corresponding resonance (J/Ψ for $c\bar{c}$ and Υ for $b\bar{b}$). Using eq. (5.2) we estimate $m_c = 1.25$ GeV and $m_b = 4.63$ GeV.

For the E_u potential the minimum value of K is 1 (see table 1 of ref. [12]) so that $l \geqslant 1$. We solve eq. (5.1) numerically, approximating the E_u potential by a

constant for $R_{6.0}/a_{6.0} \leqslant 6.0$, and by the Nambu–Goto string potential for larger values of R, with the value of the string tension obtained from the combined fit to the ground state potential [eq. (3.4)], which we have already seen to be an excellent fit to the data. Given that the E_u and A_{1u} potentials are approximately degenerate at low R-values and that the lowest value of K for the A_{1u} potential is 0 (which removes the centrifugal barrier for the lowest lying states), it is interesting to solve eq. (5.1) in the A_{1u} potential to eliminate the possibility that the lowest lying hybrid corresponds to the A_{1u} and not to the E_u potential. To this end we approximate it by a constant for $R_{6.0}/a_{6.0} \leqslant 3.5$ and by a linearly rising term for larger values of R. This parametrization provides an adequate description of the data.

For the E_u potential, hybrid meson states of all J^{PC} values are possible, except the ones corresponding to even J with $P = C$. The spectrum includes the exotic values 0^{+-}, 1^{-+} and 2^{+-} [12, 24]. The A_{1u} spectrum contains no exotics.

In table 3 [columns labelled (a)] we show our estimates for the energies of a number of meson states in the $c\bar{c}$ and $b\bar{b}$ spectrum relative to the 1S level of the A_{1g} potential. The results of table 3 confirm that the lowest lying hybrid meson corresponds to the E_u representation. Errors of ± 0.03 GeV and ± 0.04 GeV should be attributed to the E_u and A_{1u} energy levels respectively, originating from the statistical errors in the evaluation of the potentials.

The entries in table 3 [columns labelled (a)] can thus be viewed as the SU(3) *pure gauge theory predictions* for the low-lying hybrid meson spectrum using the string tension value $\sigma^{1/2} = 440$ MeV obtained from the $\rho, f, \ldots$ Regge trajectories. This is expected to give the energy levels to an accuracy of 20% in comparison with experimental values, since the same level of uncertainty is observed in the value of the β-function. As expected, the spectrum of states appropriate to the $b\bar{b}$ and $c\bar{c}$ systems in the ground state potential is in qualitative agreement with experiment, but has level spacings which are small compared to the experimental values. This discrepancy is a shortcoming of the pure gauge approximation which ignores the effects of quark loops. We shall return to this point later in this section.

The main characteristics underlying the pure gauge theory predictions for the $b\bar{b}$ and $c\bar{c}$ systems are the following:

(i) *The hybrid meson spectra are dense.* This is especially true for the hybrids corresponding to the E_u potential as a result of the flatness of this potential at low and intermediate R.

(ii) *The relative position of low-lying hybrid meson levels to the hadron production threshold depends on their quark content* (c, b *or* t). On identifying the lowest lying 1S quark model states with $J/\Psi(3100)$ and $\Upsilon(9460)$ we can obtain predictions for the hybrid meson masses. Using the pure SU(3) lattice gauge theory data we find the values 4.04 GeV for the $c\bar{c}$ system and 10.56 GeV for the $b\bar{b}$ system. While for the $c\bar{c}$ system the lowest levels lie safely above the $D\bar{D}$ meson production threshold (3.73 GeV), the corresponding $b\bar{b}$ levels are approximately degenerate with the $B\bar{B}$

TABLE 3

Energy levels of ordinary quark model and hybrid mesons corresponding to the $c\bar{c}$ and $b\bar{b}$ systems relative to the 1S quark model states [$J/\Psi(3100)$ and $\Upsilon(9460)$] calculated by solving the Schrödinger equation in the appropriate potentials. (a) Pure SU(3) gauge theory results obtained under the assumption that the physical distance scale is set by the value $\sigma^{1/2} = 0.44$ GeV. (b) Values obtained by modifying the A_{1g} potential to take account of light quark loop effects as discussed in the text, so that the levels of mesons corresponding to the A_{1g} potential agree closely with the experimental values. The experimental values for the $D\bar{D}$ and $B\bar{B}$ meson production thresholds are 3.73 GeV and 10.54 GeV respectively

Representation	n,l	$\Delta M_{c\bar{c}}$(GeV)		$\Delta M_{b\bar{b}}$(GeV)	
		(a)	(b)	(a)	(b)
A_{1g}	1P	0.38	0.43	0.32	0.45
	2S	0.59	0.63	0.45	0.56
	1D	0.68	0.74	0.54	0.70
	2P	0.87	0.93	0.66	0.81
	3S	1.06	1.10	0.77	0.91
E_u	1P	0.94	1.07	1.11	1.36
	1D	1.17	1.29	1.22	1.46
	2P	1.34	1.46	1.33	1.57
	1F	1.38	1.50	1.33	1.57
	2D	1.54	1.66	1.44	1.68
	3S	1.69	1.80	1.53	1.77
	2F	1.73	1.84	1.54	1.79
A_{1u}	1S	1.11	1.24	1.25	1.50
	1P	1.41	1.53	1.42	1.66
	2S	1.65	1.77	1.58	1.83
	1D	1.68	1.80	1.58	1.83

meson production threshold (10.54 GeV). A word is in order here about the $t\bar{t}$ hybrids. Although it is hard to determine fully the meson spectrum corresponding to the $t\bar{t}$ system (because it is very sensitive to the small R-dependence of the ground state potential), we can predict the relative position of the corresponding lowest hybrid meson to the threshold for meson production. The threshold for the $t\bar{t}$ system is expected to lie on the same horizontal line as the threshold for the $b\bar{b}$ system in the graph of fig. 2 [25]. Using a mass of 120 GeV for the top quark, we can estimate that according to the pure gauge theory the lowest lying $t\bar{t}$ hybrid meson lies below threshold, and thus it need not have a broad width. Note, however, that the full theory with dynamical fermions may reverse this result (see below).

(iii) *The partial width for the decay of the* 1^{--} *levels into* e^+e^- *is suppressed.* Indeed, for the 1^{--} levels corresponding to the E_u potential, the presence of a centrifugal barrier means that the radial wave function vanishes at the origin. There is a 1^{--} hybrid meson state with $K = l = 0$ corresponding to the A'_{1g}

potential, but the relative flatness of this potential means that the radial wave function is spatially extended. It is thus not likely that the corresponding hybrid meson states can be seen in direct electro-production.

In the pure gauge approximation, light quark loops are neglected, whose effect would be to increase the strength of the Coulomb term in eq. (3.1). In an attempt to estimate the possible effect of quark loops on our results, we accordingly increase the Coulomb strength to the value $e = 0.470$ to obtain the potential depicted by the dashed line in fig. 2. We thus essentially reproduce the parameters of the phenomenological Cornell potential [26] and obtain spectral levels in good agreement with the experimental values. This involves redefining the quark masses to comply with eq. (5.2) ($m_b = 4.75$ GeV and $m_c = 1.32$ GeV). This modification increases the difference between the energies of hybrid mesons and the lowest lying quark model meson, but it hardly affects the splitting between the hybrid levels themselves. The modified levels are listed in columns labelled (b) in table 3. String model, QCD sum rules and bag model calculation results [24, 27, 28] are in agreement with the estimates of table 3.

Allowing for the modification of the Coulomb term, the lowest hybrid meson levels are pushed up to 4.19 GeV and 10.81 GeV for the $c\bar{c}$ and $b\bar{b}$ systems respectively. The differences between these values and the pure gauge approximation values (0.15 GeV for $c\bar{c}$ and 0.25 GeV for $b\bar{b}$) should be taken as an indication of the systematic error inherent in the pure gauge approximation in relation to the full theory with dynamical fermions. Moreover, the estimated hadron production threshold for the $t\bar{t}$ system now lies below the minimum of the E_u potential in fig. 2. For all three systems ($c\bar{c}$, $b\bar{b}$ and $t\bar{t}$), the lowest hybrid meson states now lie safely above threshold, so that open channel decays will mean that these levels have broad widths. If eventual simulations of QCD with dynamical fermions confirm these estimates, J^{PC} determination experiments will remain the only reliable hope of identifying hybrid mesons, since some of these are expected to have exotic quantum numbers.

6. Conclusions

In this paper we have studied the ground state and excited potentials between a static quark–antiquark pair in the context of SU(3) lattice gauge theory without dynamical fermions. By using "blocked" links in the spatial directions we have been able to construct operators with greatly improved overlaps with the ground state of each D_{4h} representation, and hence to determine potentials to a high degree of accuracy. The E_u potential has been found to be the lowest lying excited potential and is thus the most relevant to hybrid meson phenomenology. The potentials exhibit non-perturbative scaling behaviour in the region $\beta = 6.0$–6.2 within the errors. Comparison of our results to the predictions of a relativistic

string model has shown that the latter provides an accurate description of the E_u potential for quark–antiquark separations greater than 3 GeV^{-1}.

The accuracy with which the low-lying potentials have been determined has enabled us to calculate masses of hybrid mesons with heavy quarks. We can thus claim that we have obtained an accurate picture of the low-lying hybrid spectrum as predicted by pure SU(3) lattice gauge theory. The question still remaining is to what extent this spectrum will be altered through the inclusion of dynamical quarks. Although we have tried to estimate this effect, obtaining an accurate guide for the experimentalists will probably require a simulation of the full theory.

S.P. acknowledges the financial support of SERC. C.M. wishes to thank SERC for grant GR/E 8728.1 of computer time on the CRAY XMP/48 at RAL.

References

[1] R. Sommer and K. Schilling, Z. Phys. C29 (1985) 95
[2] D. Barkai, K.J.M. Moriarty and C. Rebbi, Phys. Rev. D30 (1984) 1293
[3] J.D. Stack, Phys. Rev. D29 (1984) 1213
[4] S.W. Otto and J.D. Stack, Phys. Rev. Lett. 52 (1984) 2328
[5] K.C. Bowler et al., Phys. Lett. B163 (1985) 367
[6] J. Flower and S.W. Otto, Phys. Rev. D34 (1986) 1649
[7] A. Hasenfratz et al., Z. Phys. C25 (1984) 191
[8] N.A. Campbell, C. Michael and P.E.L. Rakow, Phys. Lett. B139 (1984) 288
[9] N.A. Campbell et al., Phys. Lett. B142 (1984) 291
[10] N.A. Campbell, A. Huntley and C. Michael, Nucl. Phys. B306 (1988) 51
[11] I.J. Ford, R.H. Dalitz and J. Hoek, Phys. Lett. B208 (1988) 286;
I.J. Ford, Oxford University preprint TP-61 (1988)
[12] S. Perantonis, A. Huntley and C. Michael, Nucl. Phys. B326 (1989) 544
[13] S. Perantonis, Nucl. Phys. B (Proc. Suppl.) 9 (1989) 249
[14] C. Michael and M. Teper, Phys. Lett. B199 (1987) 95
[15] C. Michael and M. Teper, Nucl. Phys. B314 (1989) 362
[16] G. Parisi et al., Phys. Lett. B128 (1983) 418
[17] M. Albanese et al., Phys. Lett. B192 (1987) 163; B197 (1987) 400;
L. Fernandez and E. Marinari, Nucl. Phys. B295 (1988) 51
[18] K.C. Bowler et al., Phys. Lett. B179 (1986) 375
[19] C. Michael, Liverpool preprint LTH244, Nucl. Phys. B (Proc. Suppl.) 17 (1990) 59
[20] M. Lüscher, Nucl. Phys. B180 [FS2] (1981) 317
[21] M. Caselle, R. Fiore and F. Gliozzi, Phys. Lett. B224 (1989) 153
[22] J.H. Merlin and J. Paton, Phys. Rev. D36 (1987) 902
[23] J.F. Arvis, Phys. Lett. B127 (1983) 106;
O. Alvarez, Phys. Rev. D24 (1981) 440
[24] N. Isgur and J.E. Paton, Phys. Rev. D31 (1985) 2910
[25] C. Quigg and J.L. Rosner, Phys. Rep. 56 (1979) 167
[26] K. Hagiwara, A.D. Martin and A.W. Peacock, Z. Phys. C33 (1986) 135
[27] J. Govaerts et al., Nucl. Phys. B284 (1987) 674
[28] P. Hasenfratz et al., Phys. Lett. B95 (1980) 299;
S. Ono, Z. Phys. C26 (1984) 307